

Modeling and Simulation of Monolithic AlGaAs/InGaAs Tandem Solar Cell

¹ Samia SLIMANI, ² Shanawer NIAZ, ³ Bouaza DJELLOULI

^{1,3} Department of Electronics, Faculty of Science, Laboratoire de Modélisation et Méthodes de calcul LMMC Moulay Tahar University, Saida, 20002, Algeria

² Department of Physics, University of Sargodha, 40100, Sargodha, Pakistan

¹ Tel./fax: 213 (0) 48 47 15 08

E-mail: slimani.samia@gmail.com

Received: 3 May 2015 / Accepted: 5 June 2015 / Published: 30 June 2015

Abstract: Employing conventional III-V junctions we report a classical calculation of conduction and valence band edge and the electron and hole densities. It is shown that the optimum performance can be achieved by employing AlGaAs /AlGaAs/InGaAs monolithic cascade solar cells, we have established these calculations by solving the Poisson equation within the framework of the Nextnano. Copyright © 2015 IFSA Publishing, S. L.

Keywords: Solar cell, Nextnano3d, AlGaAs /AlGaAs/InGaAs, Photovoltaic, III-V semiconductor.

1. Introduction

The advantage of solar cells fabricated by forming a monolithic crystalline stack of materials with the desired bandgaps is the simplicity in processing. The disadvantage is that there are a limited number of materials combinations which can be epitaxially grown in device quality form. The p-n junction of the one junction solar cell can only achieve high power conversion efficiencies for a limited range of photon energies lying close to the energy gap between the valence and conduction bands. In contrast, multijunction solar cells or a monolithic cascade cell are composed of tandem p-n junctions, where the bandgap of each subcell is tailored to a different range of photon energies for which much wider spectral range is obtained by multijunction solar cells.

The experimentally-measured conversion efficiencies are up to 40.7 % [1, 2] and 40.8 % [3]. The monolithic, series interconnected multi-junction (MJ) solar cells based on group III-V semiconductor material system are proven to be very attractive for many space and terrestrial applications [4, 5].

The cascade solar cells are monolithically integrated into a multi-layered device in order to conduct current between the subcells; basically is comprised of at least three layers. The layer with the largest bandgap is placed on the top and other layers are placed in the order of decreasing bandgaps, such that each layer absorbs and converts the photons with energies between its own bandgap and that of the previous layer. The tunnel layers are always more heavily-doped than the cell layers with doping concentrations typically greater than 10^{19} cm^{-3} . The tunnel layer is introduced to connect the p terminal of one subcell to the terminal of an adjacent subcell. The tunnel junction must be transparent to the wavelengths absorbed in the subsequent subcells, and it must form a low-resistance contact to ensure a minimal voltage drop.

One such standard is the Air Mass 1.5 Global (1000 W/m^2 , AM1.5G) solar spectrum [6, 7]. Although it is usually given as spectral irradiance (in units of $\text{W m}^{-2} \text{ nm}^{-1}$), it can easily be converted to spectral photon flux density (in units of photons $\text{m}^{-2} \text{ s}^{-1} \text{ nm}^{-1}$). Thus far, practical PV devices, when operated in an energy production mode, can produce

only one electron in an external circuit for every incoming photon.

Due to the importance of the tunnel junction on the overall conversion efficiency, the relationship between the quality of a tunnel junction and the semiconductor parameters used to design its structure is identified by energy band diagram and densities characteristics. This paper presents the comparison of the energy band diagram and densities characteristics for the AlGaAs/InGaAs with homojunction Al_{0.141}Ga_{0.859}As tunnel junction and AlGaAs/AlGaAs/InGaAs with two homojunction Al_{0.141}Ga_{0.859}As tunnel junction.

In this work, based on Nextnano simulator, dimensional (1D) simulation has been performed on AlGaAs/InGaAs and AlGaAs/AlGaAs/InGaAs solar cell devices. This paper is organized as follows. In Section 2, the device structure and simulation details are explained. The simulator Nextnano and basic theoretic background are briefly described in Section 3. Modeling results, analyses and discussion are presented in Section 4. Finally, a summary is given in Section 5. Good simulation software could usually help to obtain a better understanding of the performance characteristics and predict the operational condition for these solar cells.

2. Device Structure and Simulation Details

AlGaAs/InGaAs solar cells were fabricated on a GaAs substrate, based on an experimental results of US patent [6], AlGaAs and InGaAs single junction solar cells and AlGaAs tunnel junction also Possible design optimization of triple-junction (TJ) solar cell is suggested by simulation in order to enhance the efficiency starting from the bottom, the TJ solar cell is constructed with three subcells, namely AlGaAs/AlGaAs and InGaAs junctions stacked in series. An anti-reflective coating (ARC) layer is at the very top the tunnel junction is implemented and placed between two subcells. Although the actual device growth uses thin GaAs. AlGaAs layer is the first layer which is heavily doped (10^{18} - 10^{19} cm⁻³) with a 1.920 eV band at the surface graded to 1.890 eV. The top cell is p-n homojunction Al_{0.14}Ga_{0.86}As moderately doped (10^{17} cm⁻³), and exhibit 1.590 eV bandgap. n-doped AlGaAs, heavily doped (10^{18} cm⁻³), bandgap of greater than 1.62 eV, is inserted between the top cell and tunnel junction. the tunnel homojunction Al_{0.141}Ga_{0.859}As material heavily doped (10^{19} - 10^{21} cm⁻³cm) to provide a minimum 1.62 eV bandgap the heavily p-doped AlGaAs (10^{18} cm⁻³), is between the tunnel junction and bottom cell which has a bandgap lower than the bandgap of the first layer is In_{0.388}Ga_{0.612}homojunctionare moderately doped (10^{17} cm⁻³) to provide a bandgap of 0.954 eV for the second layer. The homojunction InGaAs graded material is between the bottom cell and n-doped

GaAs on which the cell has been formed. The effects of mismatch can be minimized by use of graded layers between the voltage producing layers. Solar cells are connected in a series configuration, and the device is accessed through two terminals.

Based on a modelling of dual-junction solar cells including AlGaAs tunnel junction, the triple junction AlGaAs/AlGaAs/InGaAs solar cells were established and applied to semiconductor junction including Two AlGaAs tunnel junctions are placed between each pair of subcells. Efficiencies of 30-40% can be achieved.

The reliable theoretical simulation is necessary for systematical improving, understanding or predicting the properties of semiconductor solar cell. Structures with solar cell can evince different properties depending on many parameters, such as shape, size, material of the covering layers. The simulator can generate files for mesh, material and doping information, which will be subsequently cited by the solving file for simulating the device. The geometry of the device is completely specified in the input file. Each model can be accompanied by a full set of its parameters and each material can be doped by any dopant to the desired concentration. This can be done in a regular uniform way, in a linear or even a Gaussian distribution.

3. Calculation Method

The Poisson equation is solved in an AlGaAs/InGaAs and AlGaAs/AlGaAs/InGaAs monolithic cascade solar cells, we have established a classical calculation of conduction and valence band edge and the electron and hole densities. These calculations were performed within the framework of the Nextnano3 [7] the basic Semiconductor equations is by the solving the Schrödinger, Poisson, current continuity equations for electrons and holes and the current relations for electrons and holes

The Poisson equation:

$$\nabla^2 \psi = \frac{q}{\epsilon} \cdot (n - p - c) \quad (1)$$

The current continuity equation for electrons and holes:

$$\begin{aligned} \nabla \cdot \vec{J}_n - q \cdot \frac{\partial n}{\partial t} &= q \cdot R \\ \nabla \cdot \vec{J}_p - q \cdot \frac{\partial p}{\partial t} &= -q \cdot R \end{aligned} \quad (2)$$

The current relations for electrons and holes:

$$\begin{aligned} \vec{J}_n &= q \cdot n \cdot \mu_n \cdot \vec{E}_n + q \cdot D_n \cdot \nabla n \\ \vec{J}_p &= q \cdot p \cdot \mu_p \cdot \vec{E}_p - q \cdot D_p \cdot \nabla p \end{aligned} \quad (3)$$

The charge density is calculated for a given applied voltage by assuming the carriers to be in a local equilibrium that is characterized by energy-

band dependent local quasi-Fermi levels $E_{Fc}(x)$ for charge carriers of type c (i.e. in the simplest case, one for holes and one for electrons),

$$n_c(x) = \sum_i |\psi_{ic}(x)|^2 f\left(\frac{E_{Fc}(x) - E_{ic}}{K_B T}\right) \quad (4)$$

These local quasi-Fermi levels are determined by global current conservation $\nabla \cdot J_c = 0$, where the current is assumed to be given by the semi-classical relation:

$$J_c(x) = \mu_c \cdot n_c(x) \nabla E_{Fc}(x) \quad (5)$$

The carrier wave functions ψ_{ic} and energies E_{ic} are calculated by solving the multiband Schrodinger-Poisson equation.

Our calculation results show the band edges diagram and electron and hole densities in the vicinity of the tunnel junction of AlGaAs/InGaAs monolithic cascade solar cell.

The built-in potential has been calculated to be 1.83 V at zero bias and we assumed that all materials are strained with respect to the GaAs substrate, a graded p-type AlGaAs layer has been used to generate an electric field of 3 kV/cm (=30 meV/100 nm) [8, 9].

4. Results

Most of the photons that are absorbed in the semiconductor produce such electron-hole pairs. These electron-hole pairs generate photocurrent and in the presence of a built-in field, and the photovoltage of the solar cells.

In the figures below we show as examples of our calculation results the band edges diagram and electron and hole densities in the vicinity of the tunnel junction of AlGaAs/InGaAs monolithic cascade solar cell.

Fig.1 shows the simulated band diagrams of the samples in the based layout of US patent [8]. Also the band edges diagram of AlGaAs/ AlGaAs/InGaAs monolithic cascade solar cell is showed in Fig. 2, we can see clearly that the degeneracy of heavy and light hole valence band edges is lifted, especially inside the InGaAs regions.

The band diagram around the AlGaAs layer in the structure of Fig.1 is quite similar to a tunneling junction of Fig.2 except for the area around the tunnel junction which is in the middle of the device for the first sample at ~2100 nm and for the second sample at 2100nm and 4200nm.

It is well known that photons energies in excess of the threshold energy gap or band gap between the valence and the conduction bands are dissipated as heat; thus they are wasted specifically, there is a fixed quantum of potential energy difference across the band gap in the semiconductor. The band gap of AlGaAs/InGaAs as a function of distance is shown in the following Fig.3.

Tunnel junctions play an important role in the MJ solar cells by facilitating the current transfer from one subcell to another. A thin tunnel junction could be simply created by doping either side of the junction very heavily [10]. If both sides of the junction are sufficiently doped, the conduction band and valence band may cross the Fermi level to align the electrons with empty states [11]. Energy band diagram for the AlGaAs tunnel junction at 0 V bias, where the electron and hole quasi-Fermi levels are superimposed and the depletion region is highlighted. (Fig.4).

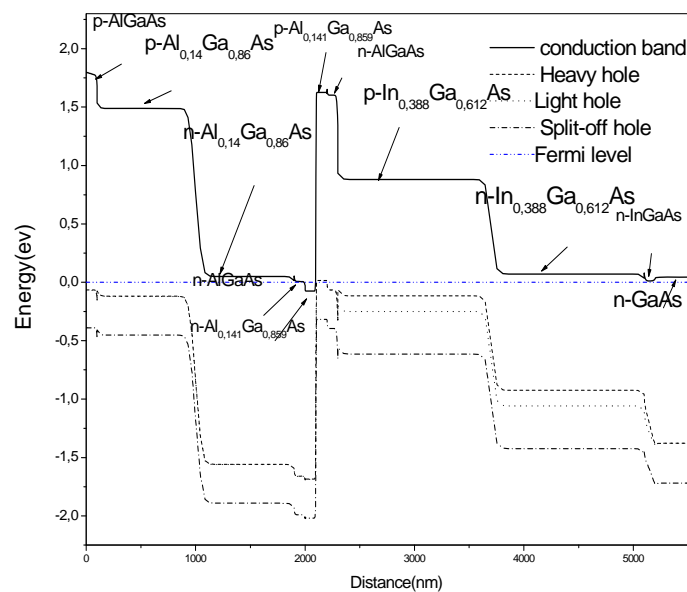


Fig. 1. Conduction band edges of AlGaAs/InGaAs monolithic cascade solar cell.

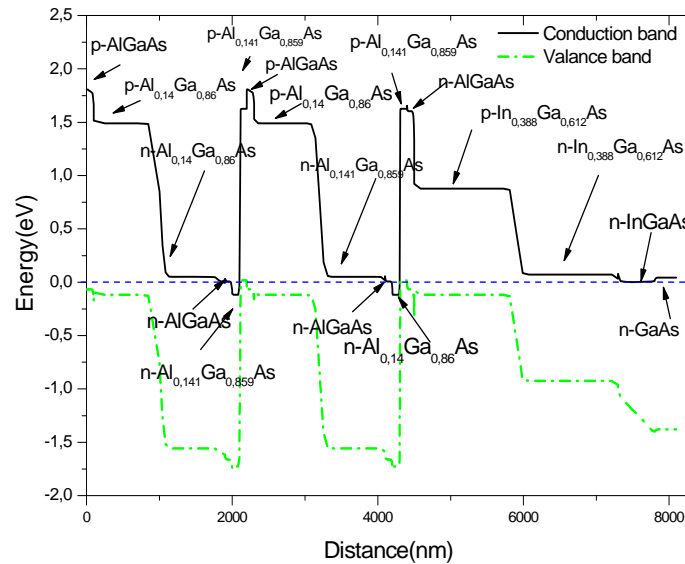


Fig. 2. Conduction band edges of AlGaAs /AlGaAs/InGaAs monolithic cascade solar cell.

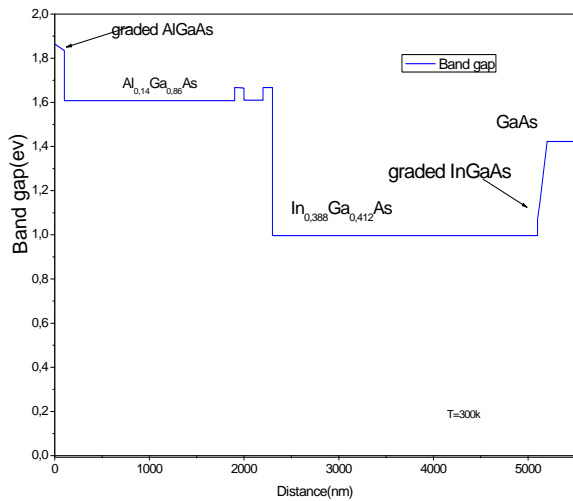


Fig. 3. Band gap of AlGaAs/InGaAs monolithic cascade solar cell [2].

The density has been calculated classically the density and the potential are calculated self-consistently from Poisson equation.

The electron and hole densities in the vicinity of the tunnel junction for the AlGaAs/InGaAs Tandem cell are shown in Fig. 5.

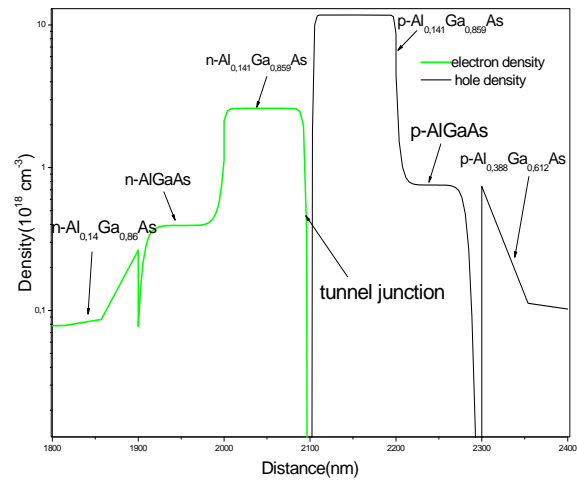


Fig.5. Electron and hole densities of AlGaAs/InGaAs monolithic cascade solar cell.

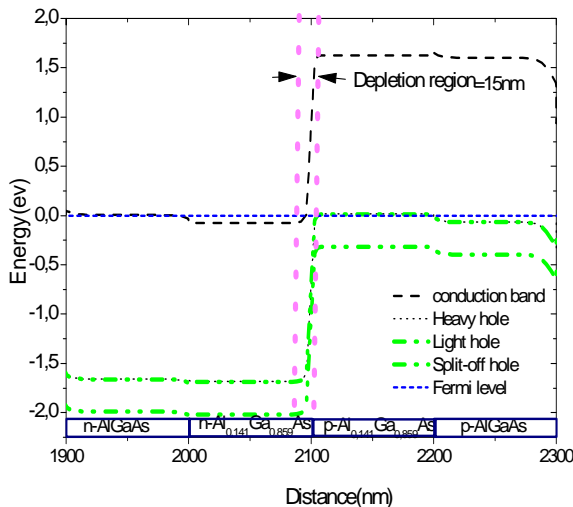


Fig.4. Depletion region of AlGaAs/InGaAs monolithic cascade solar cell.

The achievable efficiency of a solar cell material will depend on the characteristic energy bandgap of the material. Anyway, our results indicate the possibility of achieving a tunneling junction using TJ solar cell.

7. Conclusions

Designing efficient solar cells is very important, by several key criterions in designing high quality solar cells Semiconductor materials should be chosen

targeting certain wavelength of the solar radiation spectrum. This will Minimize optical losses and maximize photon absorption, reduce recombination losses in the quasi-neutral and depletion region. Implementation of III-V direct bandgap optically sensitive and form better matching (lattice, optical and electrical) between subcell layers, high carrier mobility semiconductors, form better matching (lattice, optical and electrical). The simulation software nextnano was used to help to design the monolithic cells, the implications of these two-junction or three-junction cascade solar cells to obtain maximum efficiency for terrestrial applications.

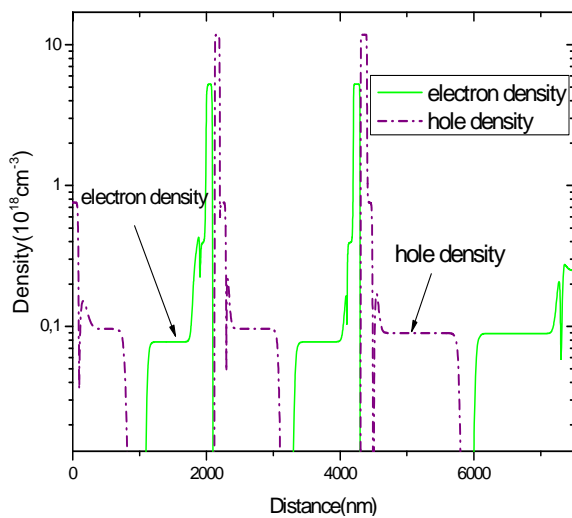


Fig. 6. Electron and hole densities of AlGaAs /AlGaAs/InGaAs monolithic cascade solar cell.

Acknowledgements

The authors would like to thank the support of the laboratory of method LLMC of Saida University and also the anonymous reviewers for their critical comments.

References

[1]. R. R. King, R. A. Sherif, D. C. Law, J. T. Yen, M. Haddad, C. M. Fetzer, K. M. Edmondson, G. S. Kinsey, H. Yoon, M. Joshi, S. Mesropian,

H. L. Cotal, D. D. Krut, J. H. Ermer, and N. H. Karam, New Horizins in III-V Multijunction Terrestrial Concentrato Cell Rerserach, in *Proceedings of the 21st European PV Solar Energy Conference*, 4-8 September 2016, Dresden, Germany.

[2]. King R. R. Fetzer C. M., Law D. C., Edmondson K. M., Yoon Hojun, Kinsey, G. S., Krut D. D.; Ermer, J.H., Hebert P., Cavicchi B.T., Karam N. H., Advanced III-V Multijunction Cells for Space in *Proceedings of the 4th IEEE World Conference on PV Energy Conversion*, Waikoloa, Hawaii, Piscataway, NJ, 2006, pp. 1757 – 1762.

[3]. J. F. Geisz, D. J. Friedman, J. S. Ward, A. Duda, W. J. Olavarria, T. E. Moriarty, J. T. Kiehl, M. J. Romero, A. G. Norman and K. M. Jones, 40.8 % efficient inverted triple-junction solar cell with two independently metamorphic junctions, *Appl. Phys. Lett.*, 93, 2008,123505.

[4]. J. M. Olson, S. R. Kurtz, A. E. Kibbler, and P. Faine, A 27.3 % efficient Ga_{0.5}In_{0.5}P/GaAs tandem solar cell, *Appl. Phys. Lett.*,56, 1990, pp. 623-625.

[5]. D. J. Friedman, S. R. Kurtz, K. A. Bertness, A. E. Kibbler, C. Kramer, J. M. Olson, D. L. King, B. R. Hansen, and J. K. Snyder, GaInP/GaAs monolithic tandem concentrator cells, in *Proceedings of the 1st World Conference on PVEC*, 1994, p. 1829.

[6]. G. Dennler, The value of values, *Mater. Today*, 10, 11, 2007, p. 56.

[7]. ASTM Standard G173, Standard Tables for Reference Solar Spectral Irradiances: Direct Normal and Hemispherical on 371 Tilted Surface, ASTM International, West Conshohocken, PA: <http://www.astm.org>, accessed on 12/14/2007.

[8]. ASTM Standard G173, Standard Tables for Reference Solar Spectral Irradiances: Direct Normal and Hemispherical on 371 Tilted Surface, ASTM International, West Conshohocken, PA: <http://www.astm.org>, accessed on 12/14/2007.

[8]. US Patent 4, 179, 70: Cascade solar cell. Lamorte; Michael F., March 9, 1978.

[9]. S. Birner, Nextnano3, next generation 3D nanodevice simulator available: <http://www.nextnano.de/nextnano3/tutorial.htm>

[10]. K. Jandieri, S. D. Baranovskii, W. Stolz, F. Gebhard, W. Guter, M. Hermle, and A. W. Bett, Fluctuations of the peak current of tunnel diodes in multi-junction solar cells, *J. Phys. D Appl. Phys.*,42, 15, 2009, 155101.

[11]. Sun, Z., Xu, S., Dai, G., Li, Y., Lou, L., Liu, Q. and Zhu, R., A microscopic approach to studying colloidal stability, *J. Chem. Phys.*, Vol. 119, No. 4, 2003, pp. 2399–2405.